Journal of Cellular Biochemistry 67:112–130 (1997)

Quantitative Immunofluorescence and Immunoelectron Microscopy of the Topoisomerase IIα Associated With Nuclear Matrices From Wild-Type and Drug-Resistant Chinese Hamster Ovary Cell Lines

Nikola I. Valkov, Jana L. Gump, and Daniel M. Sullivan*

H. Lee Moffitt Cancer Center & Research Institute, Departments of Internal Medicine and Biochemistry & Molecular Biology, University of South Florida, Tampa, Florida 33612

Abstract Topo IIα is considered an important constituent of the nuclear matrix, serving as a fastener of DNA loops to the underlying filamentous scaffolding network. To further define a mechanism of drug resistance to topo II poisons, we studied the quantity of topo IIα associated with the nuclear matrix in drug-resistant SMR_{16} and parental cells in the presence and absence of VP-16. Nuclear matrices were prepared from nuclei isolated in EDTA buffer, followed by nuclease digestion with DNase II in the absence of RNase treatment and extraction with 2 M NaCl. Whole-mount spreading of residual structures permits, by means of isoform-specific antibody and colloidal-gold secondary antibodies, an estimate of the amount of topo IIα in individual nuclear matrices. There are significant variations in topo IIα amounts between individual nuclear matrices due to the cell cycle distribution. The parental cell line contained eight to ten times more nuclear matrix–associated topo IIα than the resistant cell line matrices. Nuclear matrix–associated topo IIα from wild-type and resistant cell lines correlated well with the immunofluorescent staining of the enzyme in nuclei of intact cells. The amount of DNA associated with residual nuclear structures was five times greater in the resistant cell line. This quantity of DNA was not proportional to the quantity of topo IIα in the same matrix; in fact they were inversely related. *In situ* whole-mount nuclear matrix preparations were obtained from cells grown on grids and confirmed the results from labeling of isolated residual structures. J. Cell. Biochem. 67:112–130, 1997.

Key words: DNase II; decatenation; in situ nuclear matrix; mitotic chromosomes; VP-16; RNP

DNA topo II is an enzyme that introduces transient double-strand DNA breaks. By regulating the superhelical density of DNA, topo II is thus involved in many aspects of DNA metabolism: replication, recombination, chromosome segregation, and transcription. In addition, topo II has been identified as an intracellular target of several clinically important antitumor drugs. These specific drugs (VP-16, *m*-AMSA, doxorubicin, and mitoxantrone) inhibit enzyme religation activity and thus lead to an increase in DNA scission. In mammalian cells, two isoforms of topo II have been identified: topo IIα with a molecular mass of 170 kDa and topo IIβ with a molecular mass of 180 kDa [Drake et al., 1987]. These two isoforms differ in their antigenic, biochemical, and pharmacological properties and show different expressions during the cell cycle. While the level of topo IIβ is relatively constant during the cell cycle, topo IIα increases in S-phase, peaks in G_2/M, and rapidly decreases after mitosis. Thus, topo IIα is considered a marker of proliferating cells and is found in tissues rich in proliferating cells [Heck and Earnshaw, 1986]. Topo IIβ is found in a wide range of tissues and is reported to be specifically associated with nucleoli [Petrov et al., 1993], although recent data [Meyer et al., 1997] do not support nucleo-

Abbreviations: BSA, bovine serum albumin; CHO, Chinese hamster ovary; CSK, cytoskeleton; EDTA, ethylenediaminetetra-acetate dihydrate; kDa, kilodaltons; *m*-AMSA, 4′-(9-acridinylamino) methanesulfon-*m*-anisidide; PBS, phosphate-buffered saline; PMSF, phenylmethylsulfonyl fluoride; RNP, ribonucleoprotein; topo II, DNA topoisomerase II (EC 5.99.1.3); VP-16, 9-(4,6,-*O*-ethylidene-β-D-glucopyranosyl)-4′-demethylepipodophyllotoxin; WT, wild-type.

Contract grant sponsor: NIH, contract grant number CA 59747; contract grant sponsor: H. Lee Moffitt Cancer Center and Research Institute Funds.

*Correspondence to: Daniel M. Sullivan, 12902 Magnolia Drive, Tampa, Fl, 33612.

Received 12 March 1997; accepted 18 June 1997

lar involvement. Topo IIα has been shown to be a structural component of the nuclear matrix [Berrios et al., 1985] and chromosome scaffold [Earnshaw et al., 1985; Taagepera et al., 1993], although some nucleolar location cannot be ruled out [Fischer et al., 1993; Meyer et al., 1997]. However, the role of individual α and β isoforms as anticancer drug targets has not been completely elucidated [Danks et al., 1994].

Drug resistance to topo II poisons may be achieved by different mechanisms, which may involve quantitative or qualitative changes in topo II as well as changes in the subcellular distribution of the enzyme. Qualitative changes include mutations, alterations in ATP binding, and perturbations in modulating activities (including phosphorylation and poly(ADP)-ribosylation). Quantitative changes [Webb et al., 1991] include inactivation of a topo II allele, a decrease in the topo II mRNA level, and changes in the ratio of the two isoforms. Alterations in the subcellular distribution have been observed for truncated enzymes, which have a molecular mass of 160 kDa and lack nuclear localization signals. These truncated forms are localized to the cytoplasm [Feldhoff et al., 1994; Harker et al., 1995; Mirski and Cole, 1995].

The nuclear matrix is the insoluble protein skeleton which remains after nuclei, isolated by treating cells with detergent, are digested with nucleases and extracted with either high salt or low salt buffers. It is composed of three substructures: the peripheral lamina, the fibrogranular internal nuclear matrix, and the nucleolar skeleton. The best characterized and most stable component is the nuclear lamina, and it is the least affected by the isolation protocol employed. The internal nuclear matrix is less well defined, since it is a more dynamic and reactive structure and more constantly involved in genome functions.

There is a tremendous controversy concerning the reality of the nuclear matrix, since the procedures for its preparation may be a source of artefact [Cook, 1988; Wang and Traub, 1991; Jack and Eggert, 1992]. There is also concern whether topo II (mainly the α form) is a structural component of the nuclear matrix and chromosome scaffold [Hirano and Mitchison, 1993]. The distribution and subnuclear association of topo II with the nuclear matrix is dependent on the ionic strength of the buffers used during nuclear isolation, on the nucleases used [Meller and Fisher, 1995], and on the protein extraction procedure employed. The controversial observations about the involvement of topo II as a structural component may also be due to the presence of multiple populations of the enzyme [Swedlow et al., 1993].

The DNA fragments remaining after the nuclear matrix fractionation procedure are believed to hold the bases of the DNA loops which anchor them to the rigid matrix framework via specific proteins like topo II [Fisher, 1989; Jackson, 1991; Poljak and Kas, 1995]. Topo II is presumably covalently trapped into cleavable complexes at the putative matrix-attachment regions in the presence of topo II inhibitors. The drug-induced DNA scission results in the release of fragments the size of DNA loops or domains (50–150 kb). Thus, the involvement of the nuclear matrix [Pienta et al., 1989; Pienta and Lehr, 1993] and the nuclear architecture [Penman, 1995] in the genesis of a cancer cell phenotype and drug resistance seems very likely. Matrix-associated topo II may be the critical target of topo II inhibitors, thus defining a discrete and clinically important population of the enzyme. An attenuated amount of topo II associated with the nuclear matrix in one drug-resistant cell line has been described [Fernandes et al., 1988, 1990; Fernandes and Catapano, 1991, 1995]. The cytotoxicity of topo II inhibitors is attributed to the formation of DNA-enzyme complexes in the vicinity of the replication fork, which are located at the nuclear matrix [Qiu et al., 1996]. Establishing cell lines with a reduced quantity of nuclear matrix–associated topo II would allow further study of this possible mechanism of drug resistance to topo II poisons.

The SMR_{16} CHO cell line was selected in the presence of 1.7 μM VP-16 [for initial characterization of this cell line see Sullivan et al., 1993]. Colony-forming cytotoxicity assays demonstrated that the SMR_{16} cell line is resistant to VP-16 (35-fold), VM-26 (20-fold), doxorubicin (16-fold), m-AMSA (11-fold), and mitoxantrone (8.8-fold) and is thus cross-resistant to all classes of topo II inhibitors. The resistant cell line has been shown to contain two-thirds the amount of parental topo IIα as determined by Western blotting. However, drug-induced DNA damage, measured *in situ* by alkaline filter elution and pulse-field gel electrophoresis, was 10–12 times less in SMR_{16} CHO cells. Analysis of the topo II catalytic and cleavage activities present in nuclear extracts obtained from paren-

tal and SMR_{16} cells, as well as the activities of purified preparations of the enzymes, demonstrated no significant differences. The possibility that a nuclear matrix–associated topo II population is specifically involved in the resistance of this cell line has been explored by a quantitative study at the single matrix level by means of immunoelectron microscopy. Whole-mount spreading is the most convenient method for this estimation, since it does not rely on random slices and allows easier statistical calculations and evaluations.

MATERIALS AND METHODS

Materials

^{3}H-methyl thymidine (20 Ci/mmol) was supplied by New England Nuclear Research Products (Boston, MA). Nonidet P-40 (NP-40), Triton X-100, goat antirabbit IgG-TRITC–labeled antibody, goat antirabbit IgG–10 nm colloidal gold–labeled antibody, and etoposide (VP-16) were from Sigma Chemical Co. (St. Louis, MO). DNase I and DNase II were obtained from Worthington Biochemical Co. (Freehold, NJ). Glutaraldehyde solution and 400 mesh nickel grids were provided by Electron Microscopy Sciences (Fort Washington, PA). Charged Superfrost Plus slides and formaldehyde solution were from Fisher Scientific (Pittsburgh, PA). Horseradish peroxidase–labeled donkey antirabbit antibody was purchased from Amersham Life Science Inc. (Arlington Heights, IL). Vectashield (antifade mounting medium with DAPI) was provided by Vector Laboratories Inc. (Burlingame, CA).

Tissue Culture

SMR_{16} and WT CHO cells were grown in monolayer culture in αMEM (GIBCO, Grand Island, NY), supplemented with 5% fetal bovine serum (Hyclone Laboratories, Logan, UT), penicillin (100 IU/ml), and streptomycin (100 µg/ml) (GIBCO) at 37°C in the presence of 5% CO_2 to a cell density of 4×10^4 cells/ml, as counted by trypsinizing an identical flask (total of 30 ml in 75 cm^2 flasks). DNA was labeled by the addition of 0.1 µCi/ml ^{3}H-methyl thymidine for 24 h. When drug was used, VP-16 was added for the last 1 h to the media at a concentration of 25 µM. Cells were scraped from the flasks and processed further by either the DNase I method or DNase II method for matrix preparation.

DNase I Method for Nuclear Matrix Preparation

Log-phase cells (3×10^8 total) were pelleted and washed once with PBS by centrifugation at 1,500*g* for 10 min at 4°C. The cells were swollen in 20 ml of buffer 1 (10 mM Tris/HCl, pH 7.5, 10 mM NaCl, 3 mM $MgCl_2$, 1 mM PMSF, 4 mM DTT) for 20 min. Cell lysis was performed by the addition of 2 ml 10% NP-40 (final concentration 1%), and after 15 min on ice the suspension was Dounce homogenized with 20 strokes. Nuclei were pelleted by centrifugation at 1,500*g* through a layer of 2 ml 0.25 M sucrose in buffer 1 (minus DTT). The nuclei were resuspended in 1 ml of buffer 1 and digested with 100 µg/ml RNase-free, protease-free DNase I for 40 min at 25°C. Digested nuclei were pelleted through a layer of 2 ml 0.25 M sucrose in buffer 1 as above. The pellet was resuspended in 2 ml of buffer 1 and kept on ice. The salt extraction of proteins was accomplished by the dropwise addition of an equal volume of buffer 2 (4 M NaCl, 20 mM EDTA, 20 mM Tris/HCl, pH 7.5, 2 mM PMSF) over a 2 h period on ice. The suspension was centrifuged at 2,500*g* for 15 min through a layer of 0.25 M sucrose in buffer 2, and the matrix pellet was resuspended in H_2O, pH 9 (adjusted with borate buffer), and either immediately processed for electron microscopy or frozen at −20°C for immunoblotting.

DNase II Method

Log-phase cells (3×10^8 total) were pelleted by centrifugation at 700*g* for 5 min at 4°C. The cells were washed twice in 10 ml of ice-cold solution A (0.25 M sucrose, 5 mM EDTA, 1 mM PMSF, pH 8.0) and allowed to swell in 4 ml of solution B (0.15 M sucrose, 2.5 mM EDTA, 1 mM PMSF, pH 8.0) for 15 min at 4°C. Cell lysis was accomplished by adding 200 µl 10% NP-40 (final concentration 0.5%) and gently triturating the cells by wide-mouth pipeting. After 10 min on ice, the nuclei were purified by carefully overlaying them on 2 ml of solution C (0.25 M sucrose, 0.1 mM EDTA, 1 mM PMSF, pH 6.8) and pelleting them at 1,200*g* for 10 min at 4°C. The nuclei were resuspended in 250 µl of solution C, and DNase II (commercial stock solution 37 U/µl) was added to a final concentration of 4 U/ml with digestion for 45 min at room temperature. Digested nuclei were pelleted through 1 ml of solution A by centrifugation at 1,200g for 10 min at 4°C and resuspended in 0.5 ml of solution A. A solution of 4 M NaCl, 10 mM EDTA, pH 7.2, was added dropwise over 2 h on

ice to give a final concentration of 2 M NaCl. The matrices were isolated by overlaying them on 1 ml 0.35 M sucrose/2 M NaCl, followed by centrifugation at 2,200*g* for 10 min at 4°C. The pellet was resuspended in 200 µl of solution B and stored at −20°C after mixing with an equal volume of 100% glycerol.

Western Blot Analysis

Nuclear matrices obtained from 3×10^8 cells by the DNase I and DNase II procedures above were resuspended in 200 µl of 4 mM DTT in H_2O, pH 9.0 (adjusted to pH 9.0 with 0.1 M borate buffer, pH 9.1), and frozen at −20°C. Solubilization of matrix proteins was facilitated by briefly sonicating thawed matrices with a Branson Sonifier 250 (output at microtip limit, 50% duty cycle) for 20 s (Branson Ultrasonics, Danbury, CT). The protein concentrations were determined, the samples were adjusted to equal protein amount in 100 µl volume, and finally 34 µl of 4× SDS-PAGE sample buffer (8% SDS, 400 mM DTT, 40% glycerol, 0.003% bromophenol blue) was added and the samples boiled for 2 min. Then 100 µg protein/lane was electrophoresed in a 7.5% SDS-PAGE gel and transferred to a PVDF membrane (Bio-Rad Laboratories, Hercules, CA). Anti-topo IIα rabbit antibody 454 was diluted 1:5,000 in Tris-buffered saline containing 0.05% Tween-20 and incubated with the PVDF membrane for 1 h [Sullivan et al., 1989]. The bound primary antibody was visualized by using horseradish peroxidase–labeled donkey antirabbit antibody (Amersham) diluted 1:10,000 in Tris-buffered saline and 0.05% Tween-20.

Immunoelectron Microscopy of Whole-Mount Nuclear Matrix Spreads

The isolated matrices (10 µl suspension, corresponding to approximately 10^6 residual structures) were allowed to swell for 10 min on ice in 200 µl H_2O, pH 9 (adjusted to pH 9.0 with 0.1 M borate buffer, pH 9.1). A 15 µl aliquot was layered over a 25 µl cushion of 0.25 M sucrose, 0.1% glutaraldehyde in H_2O, pH 9, in a microchamber, with carbon-coated Formvar 400 mesh nickel grids on the bottom. The microchambers were gently spun for 10 min at 200*g* at 4°C [Miller and Bakken, 1972]. The grids were floated sequentially on drops of solutions as follows. First, the grids were treated for 15 min with 1% glycine in PBS with several changes of 50 µl drops. Rabbit polyclonal antibody 454 against topo IIα was diluted 1:100 in 1% BSA in PBS, and the grids were incubated on 50 µl drops of this primary antibody at room temperature for 45 min. After three washes of 10 min each with 0.2% Triton X-100 in 1% BSA in PBS, the grids were incubated with goat antirabbit IgG–10 nm colloidal gold diluted 1:30 in 1% BSA in PBS for 25 min at room temperature. In order to minimize the nonspecific binding of secondary antibody, we preincubated an aliquot of the sample with the diluted gold-labeled antibody for 15 min and then centrifuged for 15 s at 13,000*g*; the resulting supernatant was used for the labeling [Birrell et al., 1987]. After three washes of 10 min each with 0.2% Triton X-100 in 1% BSA in PBS, the grids were rinsed several times with PBS and water and finally stained with 1% phosphotungstic acid in 70% ethanol. Grids were examined by a Philips CM 10 electron microscope at an accelerating voltage of 60 kV.

In Situ Nuclear Matrix Preparation

Formvar and carbon-coated 400 mesh nickel grids were ethanol- and UV-sterilized in petri dishes and WT and SMR_{16} cells grown on them to log-phase densities. The grids were briefly rinsed with PBS to remove media, washed for 30 s in cytoskeleton (CSK) buffer (0.3 M sucrose, 10 mM Tris/HCl pH 7.4, 100 mM NaCl, 3 mM $MgCl_2$, and 1 mM PMSF) and quickly permeabilized for 45 s in CSK buffer containing 0.5% Triton X-100. The cells attached to the Formvar grids were fixed for 1 min by incubation in drops of 2% formaldehyde/0.2% glutaraldehyde in CSK buffer. The fixation was terminated by transfer to 1% glycine in CSK buffer, followed by incubation in several drops of CSK buffer containing 0.5% Triton X-100. For a comparable nuclear matrix preparation, the DNase II procedure was followed, except that the cells were treated on drops as the grids were transferred. Briefly the grids were floated onto several drops of solution A, followed by several transfers in solution C. DNase II (37 units/ml in buffer C; 1,000 dilution from the commercial stock solution) was finally used to digest chromatin for 1 h at room temperature. The extraction with 2 M NaCl/10 mM EDTA, pH 7.2, was performed by gradually increasing the salt concentration. After the grids were rinsed with CSK buffer, residual structures were postfixed for 10 min with 0.1% glutaraldehyde, and immunolabeling was performed as described above.

The resolution of the whole-mount labeling was optimized by brief staining with 0.1% uranyl acetate dissolved in water instead of 1% phosphotungstic acid in ethanol.

Immunofluorescence Microscopy

Charged Superfrost Plus slides were rinsed in ethanol, dried, and UV-sterilized in petri dishes. WT and SMR_{16} cells were grown on the slides to a log-phase density of 5×10^5/ml (counted by trypsinizing the monolayers). The slides were rinsed briefly in PBS and fixed at −20°C with methanol/acetone (3:1). The suspension of matrices was dropped onto charged microscope slides, and, after allowing attachment for 5 min, it was fixed at −20°C with methanol/acetone (3:1) for 20 min.

The slides were air-dried and rehydrated for 2 h in several changes of PBS. Rabbit polyclonal antibody 454 against topo IIα was diluted 1:100 with 0.1% NP-40 in 1% BSA in PBS and applied to the slide for 1 h at room temperature. After several washes with PBS for 2 h, the slides were incubated with goat antirabbit IgG-TRITC–labeled antibody diluted 1:80 in 0.1% NP-40 in 1% BSA in PBS for 25 min at room temperature. After several washes in PBS, the slides were covered with coverslips in mounting media of antifade/DAPI. Immunofluorescence was observed with a Leitz (Wetzlar, Germany) Orthoplan 2 microscope, and images were captured by a CCD camera with the Smart Capture program (Vysis, Downers Grove, IL).

Statistical Methods

When DNA was quantified by using ^{3}H-methyl thymidine, 3×10^8 cells from each cell line were labeled, and in the course of nuclear matrix preparation duplicate 200 µl aliquots were withdrawn from the resultant supernatants, mixed, and counted with 2 ml of Scinti-Verse II (Fisher Scientific). One-half (100 µl) of the suspension of nuclear matrices was used for radioactivity counting, the other half for whole-mount electron microscopy (EM) spreading with immunolabeling. The radioactivity released in the supernatant by treatment with DNases and 2 M NaCl, as well as the residual DNA in nuclear matrices, was evaluated by using the paired Student *t*-test. Data from 12 separate experiments performed with equal cell numbers were analyzed. The quantity of topo IIα/matrix was determined by directly counting the colloidal particles on the photographic prints of 300 individual matrices for each cell line, and the numbers were evaluated by the paired *t*-test (GraphPad Prism 2.0; GraphPad Software Inc., San Diego, CA). The measurement of immunofluorescent intensity of nuclear and cytoplasmic compartments of 200 individual cells from each cell line at four different cell densities was repeated in three separate experiments. The fluorescence was measured for separate surface areas in pixels with the help of the Smart Capture program, and statistical analyses were performed by the paired *t*-test.

RESULTS

Nuclear Matrix Preparations From WT and SMR_{16} CHO Cells by Means of Two Different Nuclease Protocols

A comparison of nuclear matrix preparations obtained by the DNase I and DNAse II methods demonstrates the superiority of the second procedure, primarily due to the highly reproducible and well-preserved morphology of the residual nuclear matrices (Fig. 1a,b). The DNase II procedure lacks any divalent cations that could potentially activate endogenous nucleases, proteases, and phosphatases. This allows the digestion of genomic DNA to be carried out under strictly controlled conditions, with minimal amounts of nuclease, as the digestion solution is in the range of the pH optimum of the nuclease. The differences in chromatin structure between the two cell lines, as revealed by digestion with nucleases, are well defined and highly reproducible only with DNase II.

By using DNase II we established that the chromatin of SMR_{16} cells is approximately four times more resistant to nuclease digestion than the chromatin of WT cells (Table I). This is shown not only by the difference in quantity of DNA which remains attached to the nuclear matrix (1.2% and 4.4% for WT and SMR_{16} matrices, respectively; $P = 0.0116$) but is also manifested by the different quantity of ^{3}H-label released in the supernatants from nuclei after the nuclease treatment, which gives consistent values even with a 4-fold difference in nuclease concentrations. Treatment with 25 µM VP-16 for 1 h did not result in any substantial change in the chromatin of either cell line, and hence the quantity of DNA associated with nuclear matrices is the same as the control WT and SMR_{16} lines. At the level of single nuclear matrices, the quantity of associated DNA was different, varying from totally devoid of DNA to ma-

trices with large halos. The DNA quantity at the single matrix level was followed by electron microscopy (Fig. 2a,b) and fluorescence microscopy. Our evaluations suggest that in both cell lines the derived nuclear matrices are represented by both DNA-rich and DNA-poor residual structures. The difference is their proportion in the bulk suspension; DNA-rich matrices are nearly 80% of the matrices in the SMR_{16} preparation, while in the WT preparation they account for only 3–4%. Nuclear matrices prepared by the DNase I procedure did not vary in the amount of associated DNA, perhaps due to the excess of enzyme used or activation of endogenous nucleases.

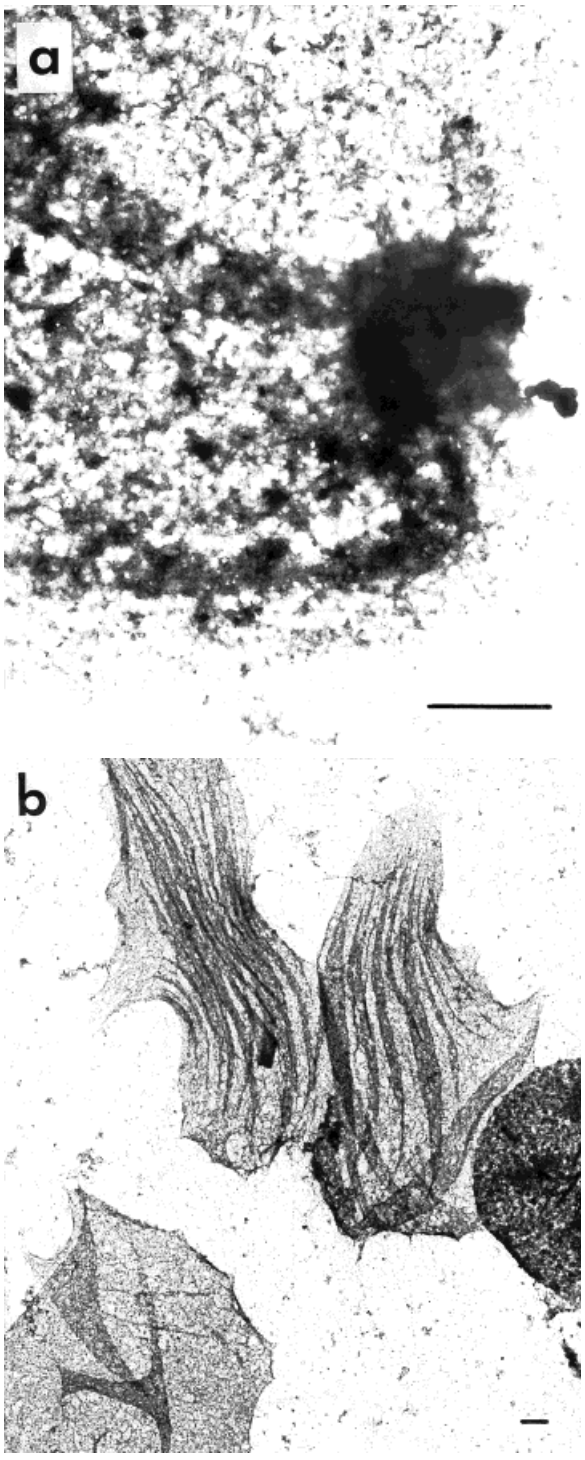

By means of electron microscopy of whole-mount spreads of isolated nuclear matrices, we observed significant differences between individual matrices in the specimens from both cell lines. The heterogeneity of individual nuclear matrices is observed not only in the shape (roundish, spindle-like, or elliptical) and dimensions (from 4–15 μm) but also in the different structure of the internal fibrogranular scaffolding network, including the density of fibrils, the structure of anastomosing meshwork, the density of associated granules, and the dimensions of granular and trabecular units (Fig. 2c). This heterogeneity within a cell line is probably related to the phase of the cell cycle from which the matrices were obtained and reflects the nuclear phenotype of different transcriptional and metabolic states of the cells. It was difficult for us to attribute a given morphological pattern of nuclear matrix to a specific phase of the cell cycle. In addition to the morphologic heterogeneity within a specific cell line, we observed marked differences in matrix structures between the WT and drug-resistant cell lines. These differences do not reflect an altered cell cycle distribution, as flow cytometry demonstrated a similar distribution for both [Sullivan et al., 1993]. The evaluation of 600 individual structures demonstrated that WT nuclear matrices have a granular appearance in 80% of the residual karyoskeletons, while SMR_{16} matrices are fibrillar in appearance 75% of the time. In

Fig. 1. Electron micrographs of whole-mount Miller spreads of nuclear matrices isolated in suspension by the DNase I and DNase II procedures. The low magnification views show one typical nuclear matrix obtained by the DNase I procedure (**a**) and four individual nuclear matrices from the DNase II procedure (**b**), all from log-phase SMR_{16} CHO cells. Note the differences in the shape, dimensions, and electron density of the internal structure between the individual nuclear matrices (b). The spindle-like shape of some nucleoskeletons is representative of the shape of the nuclei from which the matrices are derived, thus confirming the superior preservation utilizing the DNase II procedure; a well-preserved nuclear lamina layer which constrains the internal matrix meshwork. Scale bars represent 1 μm.

TABLE I. Preparation of Nuclear Matrices From WT and SMR_{16} CHO Cells by the DNase I and DNase II Methods[†]

	WT	WT + VP-16[a]	SMR_{16}	SMR_{16} + VP-16[a]
DNase I protocol				
DNA released by 100 µg/ml DNase I (%)	56.8	54.8	66.5	66.1
DNA released by 2 M NaCl (%)	42.9	44.9	33.4	33.5
Residual DNA in nuclear matrix (%)	0.3	0.3	0.1	0.4
DNase II protocol				
DNA released by				
4 U/ml DNase II (%)	19.1	17.9	10.9	11.4
16 U/ml DNase II (%)	46.3	51.7	26.5	21.7
DNA released by				
2 M NaCl/4 U DNase II (%)	79.8	81.1	84.7	84.1
2 M NaCl/16 U DNase II (%)	52.5	47.3	69.2	73.8
Residual DNA in nuclear matrix (%)	1.2 ± 0.3	1.0 ± 0.2	4.4 ± 0.7*	4.5 ± 0.6
Matrix radius (µm)[b]	5.6 ± 1.0	5.5 ± 1.2	6.7 ± 0.7	6.6 ± 1.4
Surface area (μm^2)	105 ± 42	100 ± 40	150 ± 37	149 ± 51
Topo IIα/matrix[c]	1,536 ± 350	946 ± 518	215 ± 95*	945 ± 810

[†]Isolated nuclei were treated sequentially with DNase followed by 2M NaCl. The amount of DNA released or retained was determined by labeling cells with ^{3}H-methyl thymidine for 24 h prior to the experiment.
[a]Cells were exposed to 25 µm VP-16 for 1 h immediately before isolation of nuclei.
[b]Determined by measuring the radius of 100 matrices using electron micrographs from four matrix preparations.
[c]Determined by counting 10 nm colloidal gold particles on electron micrographs of 150 matrices for each experimental point from four separate matrix preparations.
*$P < 0.02$ compared with WT matrices without VP-16.

addition, the shape was a distinctive parameter; WT matrices are precisely geometrically round-shaped, while 85% of SMR_{16} matrices are predominantly spindle-like with elliptical nucleoskeletons. The most characteristic difference was the size, as nuclear matrices from SMR_{16} cells were 50% larger as measured by the mean value of the surface area. Drug treatment with VP-16 did not change the size of nuclear matrices from either cell line. These distinct features were only seen with the DNase II procedure, as it preserves a well-defined nuclear lamina layer and yields a good resolution of the internal nuclear matrix.

Topo IIα Associated With the Nuclear Matrix in WT and SMR_{16} CHO Cells

Immunoelectron microscopy performed on spread matrices demonstrated a different amount of topo IIα in individual matrices, measured as the number of colloidal gold particles (Fig. 3a). The diversity of labeling pattern between the individual nucleoskeletons required a large statistical evaluation in order to obtain representative mean values (Table I). The significant variation between single matrices from the same cell line (hundred- to thousandfold) most likely reflects the cell-cycle-dependent differences in topo IIα quantity, as topo IIα is much more abundant during log-phase growth and increases during S-phase to peak in G_2/M [Sullivan et al., 1987; Burden et al., 1993]. Different components of the internal nuclear matrix structure were labeled with different intensity, especially some granules (Fig. 3b,c). Such heavily labeled granules were found only in nuclear matrices from WT cells and might be a characteristic feature. The remaining matrix-associated DNA showed some local clustering of topo II along the fiber's length (Fig. 3d) but not exactly at the bases of the DNA fibers, where they contact the nuclear matrix.

The quantitative estimation of topo IIα is based on the number of colloidal gold particles coupled to the secondary antibody, thus reflecting the number of bound primary antibodies to the antigen. In an isolated substructure there are no steric hindrances to antigen accessibility. Our control experiments clearly exclude the possibility of nonspecific binding under the experimental conditions we employed. Thus, we assume a direct correlation of colloidal gold particles to molecules of topo IIα in the individual matrices. The counting of colloidal gold particles was carried out on pictures at a magnification of 30 000, so 10 nm colloid could be easily seen. In cases where the picture could not accommodate the whole matrix, a represen-

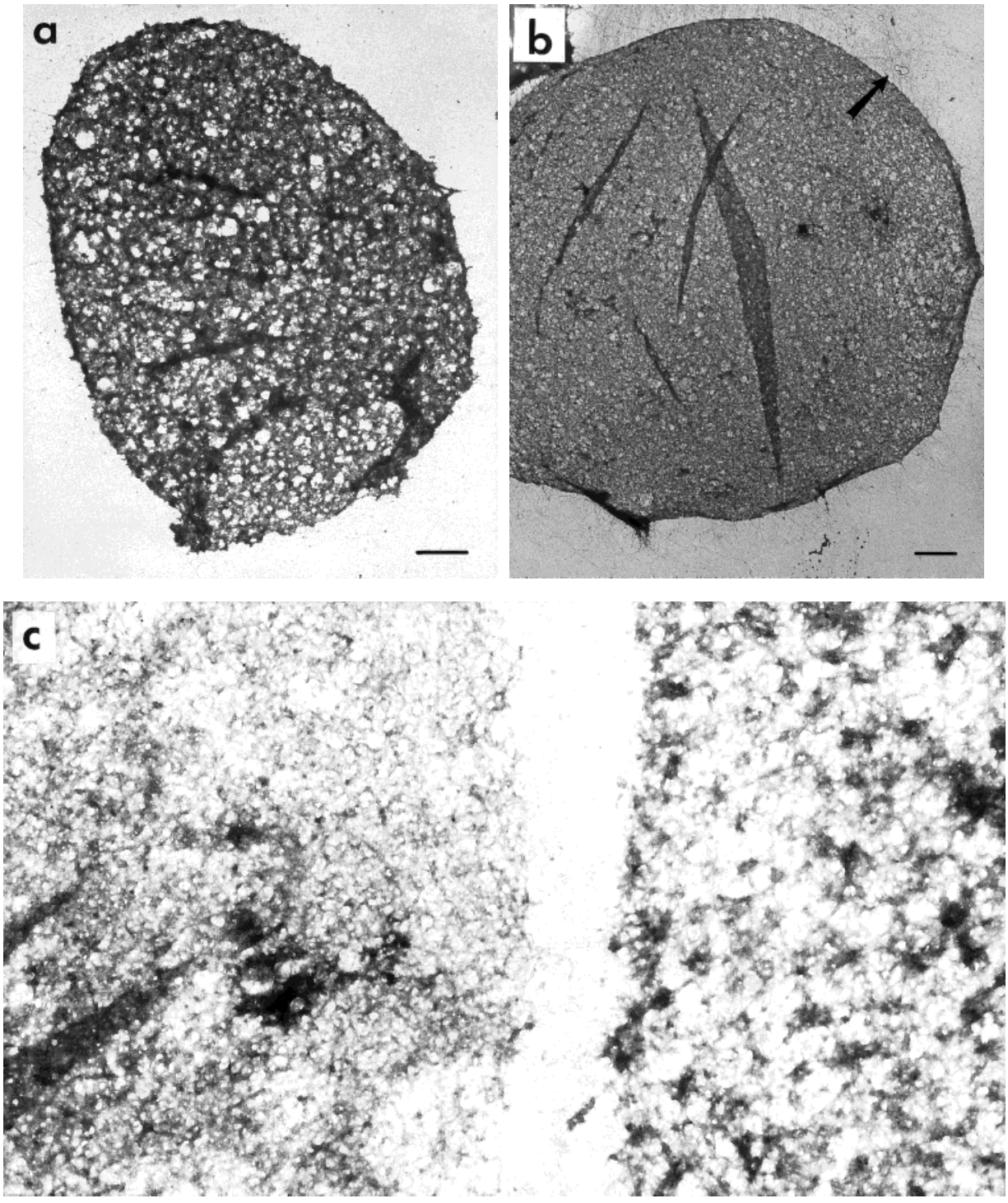

Fig. 2. Electron micrographs demonstrating the differences in the quantity of DNA associated with individual nuclear matrices obtained from the same DNase II preparation of SMR_{16} CHO cells. **a:** A nuclear matrix with essentially no residual DNA, as judged visibly by the absence of any fibers in the residual cage. **b:** A nuclear matrix with a large halo of DNA (arrow) surrounding the nucleoid. **c:** Micrograph illustrating the differences in the internal nuclear matrix structure between individual matrices derived from WT CHO cells prepared by the DNase II method. Some of the matrices have a more dense fibrillar meshwork (left), while others have a more granular appearance with thicker fibrils (right). Scale bars represent 1 μm.

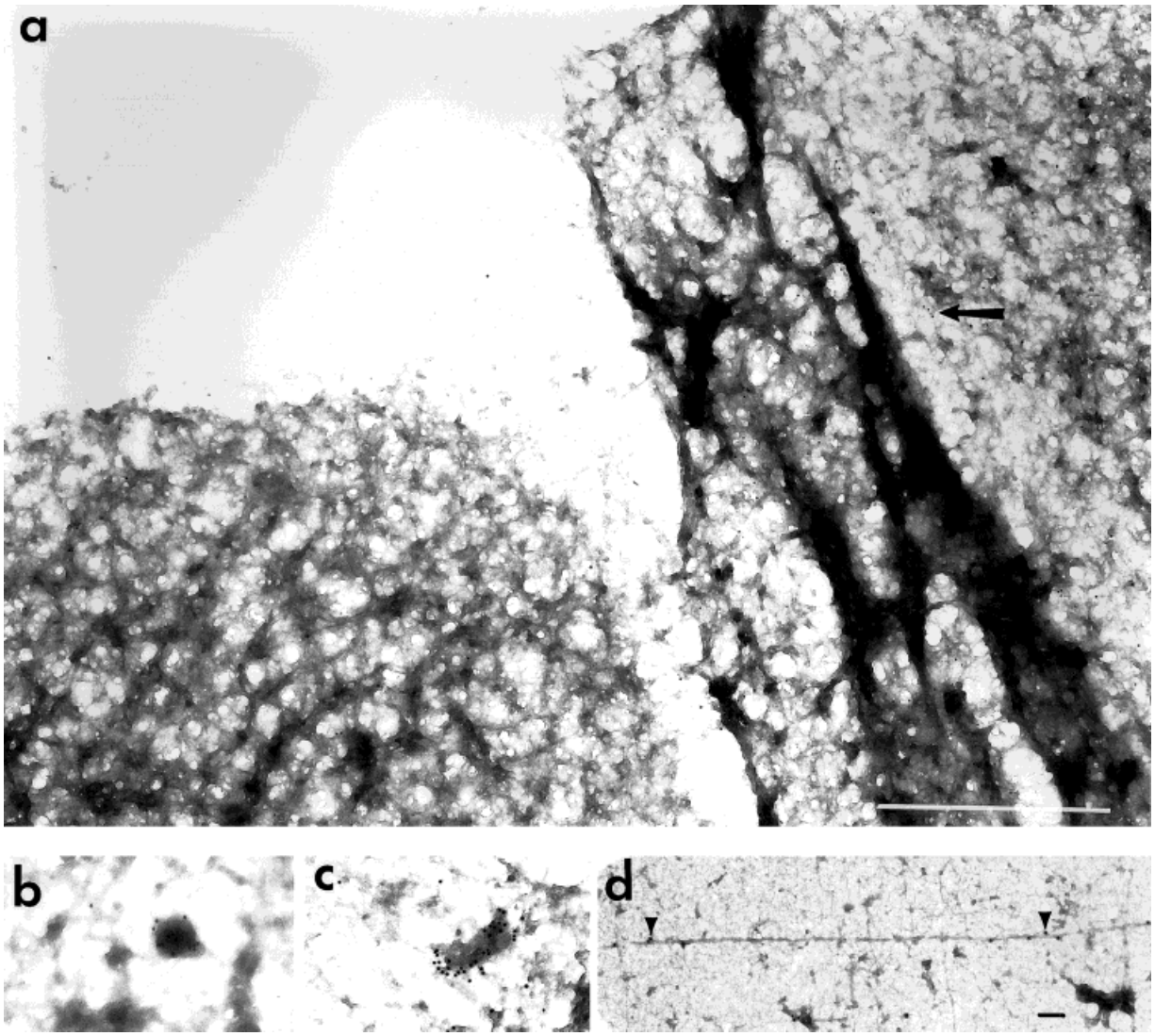

Fig. 3. Electron micrographs demonstrating the differences in the immunolabeling pattern of individual nuclear matrices derived from WT CHO cells by the DNase II method, reflecting differences in the amount of topo IIα. **a:** The residual structure on the right side is more heavily labeled (arrow) than the left one. The association of topo IIα with different components of the internal nuclear matrix—for example, with well-defined granules (**b,c**)—is quite characteristic of WT nuclear matrices. Each such granule is decorated by 16–32 10 nm colloidal gold particles. The aggregates of colloidal gold along DNA fibers reflect attached topo IIα molecules (arrowheads), but these were not found at the bases of DNA loops (**d**). a: Scale bar represents 1 μm. b-d: Scale bar represents 0.1 μm.

tative area was counted and data calculated for the entire surface area. All such calculations were routinely double-checked by counting all particles at a lower magnification. Measurements of radius and surface area were taken from the pictures. Data for each experimental point were taken from at least 100 pictures of matrices.

Topo IIα is seven- to 8-fold attenuated in matrices from SMR_{16} CHO cells compared to the WT parental line (Fig. 4a,b; Table I, where $P = 0.0198$ for WT topo IIα/matrix vs. SMR_{16} topo IIα/matrix). Treatment with VP-16 elicited a differential response, lowering the amount of topo IIα in matrices from drug-treated WT cells while increasing the amount of topo IIα associated with nuclear matrices obtained from drug-treated SMR_{16} CHO cells.

The electron microscopy findings and statistical evaluation of individual nuclear matrices were confirmed unequivocally by Western blot analyses, which demonstrated at least 5-fold more topo IIα in bulk nuclear matrices obtained by the DNase II procedure from the parental

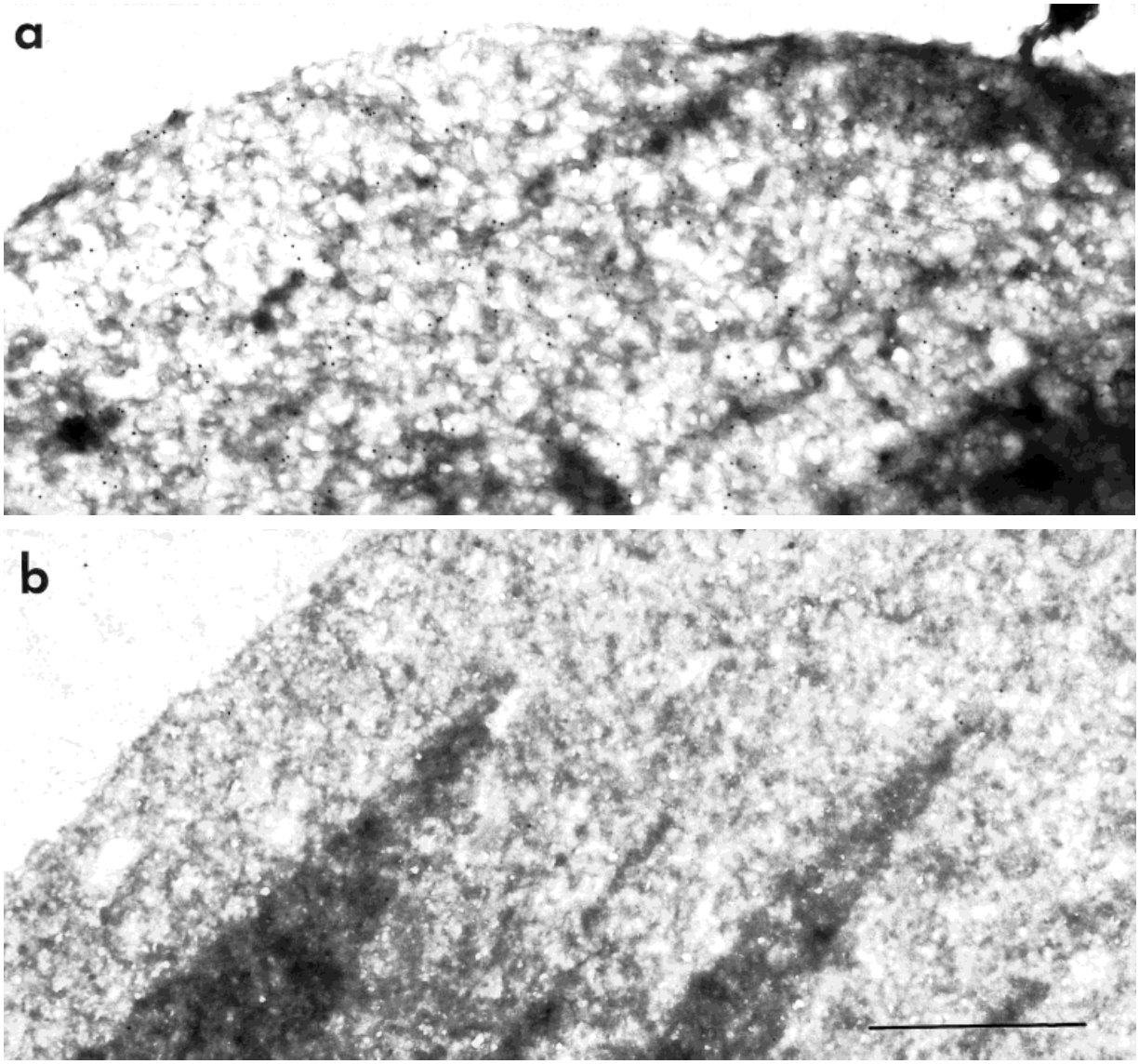

Fig. 4. Comparison of the characteristic labeling patterns of nuclear matrices for topo IIα of WT (**a**) and SMR_{16} (**b**) matrices obtained by the DNase II method. These typical residual structures represent approximately 80% of the matrices observed for the two cell lines. WT matrices are more granular and extensively labeled, while SMR_{16} matrices are more fibrillar with greatly reduced labeling. Scale bar represents 1 μm.

cell line compared to drug-resistant matrices (Fig. 5c). A similar depletion of topo IIα in drug-resistant matrices was also observed with the DNase I procedure for matrix preparation (Fig. 5a).

A major advantage of the DNase II procedure is that it allows one to measure the catalytic activity of topo II by the decatenation assay in all of the fractions separated in the course of nuclear matrix preparation. A pH of 7.4 and the addition of divalent cations totally inhibits this acidic nuclease such that it will not interfere with the decatenation assay (data not shown). The DNase I method is incompatible with measuring topo II activity, as some residual exogenous nuclease activity is always artifactually associated with the nuclear matrices and is inhibited only by the addition of large amounts of actin, which binds and inactivates the enzyme (data not shown). By using DNase II preparations, we detected topoisomerase II activity, as measured by the decatenation of kDNA, in the fractions released by the nuclease and in the high salt extract but not in the nuclear matrix fraction from either cell line (data not shown). Even large amounts of nuclear

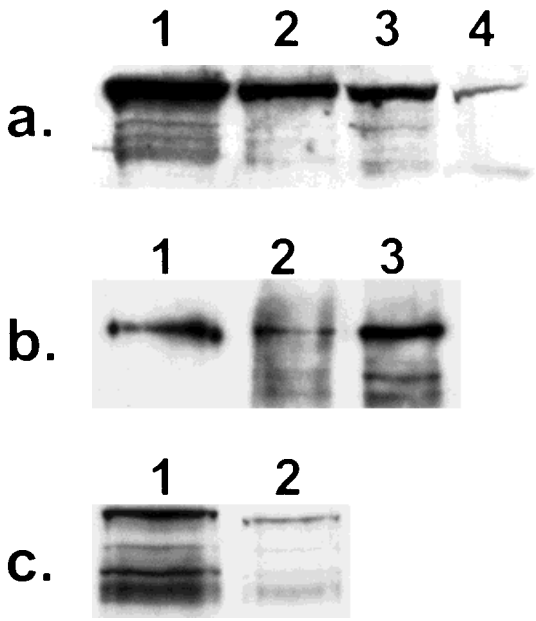

Fig. 5. Immunoblotting of nuclear matrix fractions obtained either by the DNase I (**a**) or DNase II procedure (**c**) with WT and SMR_{16} cells. The quantity of topo IIα released by 2 M NaCl is very similar for both cell lines (see **lanes 1, 2** in panel a), while the nuclear matrix fractions from WT (**lane 3**) and SMR_{16} cells (**lane 4**) show a significant difference. Similar results were obtained by the DNase II procedure (**c**), where the resistant cell line matrices (**lane 2**) were found to have at least 5-fold less topo IIα than WT cell matrices (**lane 1**). The dependence of topo II association with the nuclear matrix on RNase (**b**) is demonstrated with WT matrices. RNase treatment leads to depletion of matrix-associated topo IIα (**lane 2**) when compared to untreated WT matrices (**lane 3**). Purified topo IIα (500 ng) (**lane 1**) served as a marker and for quantitation of the signal. All lanes were loaded with 100 µg protein and after SDS-PAGE separation were transferred to PVDF membranes and detected with specific polyclonal antibody 454 against topo IIα.

matrix protein failed to demonstrate any topo II activity. We attribute this lack of enzyme activity to a very tight association of topo IIα with the insoluble matrix meshwork that is not disrupted even by sonication in the presence of 40 mM DTT. In addition, treatment with RNase did not release any active enzyme from the nuclear matrix. Thus, experimental efforts to demonstrate topo II activity in nuclear matrices were not successful.

RNase Sensitivity of Nuclear Matrix–Associated Topo IIα

The DNase II procedure has been employed largely for the isolation of nuclear lamina fractions which lack an internal nuclear matrix; this procedure is routinely carried out with RNase treatment. Since RNase digestion may disrupt the RNase-sensitive nuclear matrix fibrils or particles, we compared the DNase II isolation procedure with and without RNase treatment. It was not possible to preserve the internal fibrogranular nuclear matrix structure in the presence of RNase, as judged by electron microscopy. Perhaps the granules which are highly topo IIα–labeled are also RNP. Immunoblotting demonstrated that the quantity of topo IIα associated with the nuclear matrix is dependent on the presence of RNA, as treatment with RNase leads to a 12.5-fold reduction in immunoreactive protein associated with the salt-resistant remnant in WT matrices (Fig. 5b). This attenuation of topo II associated with the nuclear matrix from WT cells by the treatment with RNase suggests that the difference in topo IIα content between nuclear matrices from WT and SMR_{16} could be due to a lack of RNP stabilizing particles in the drug-resistant cell line. SMR_{16} nuclear matrices, which already have a significant reduction in matrix-associated topo IIα, had no further decrease in immunoreactive topo IIα by treatment with RNase.

In Situ Nuclear Matrix Preparation

In order to avoid a possible redistribution of topo II as an artefact of the isolation procedure, we developed an in situ nuclear matrix protocol for cells grown on EM grids. Very short-term fixation was employed so that the spatial relationship would be preserved. The requirement for prefixation was strengthened by the need to keep cells attached to the substrate, since the detergents used for permeabilization detach cells. The carbon film appears to be a good substrate for the cells to grow on independent of its hydrophobic properties (Fig. 6a). We adapted the DNase II procedure for the *in situ* preparative approach, and, after successfully repeating previous studies performed with DNase I [Fey et al., 1986; Chew et al., 1993], we propose an alternative DNase II method for *in situ* nuclear matrix studies. Our method seems to give a representative image of the nuclear architecture that can be compared to the images obtained by resinless thin sections and has the advantage of preserving the overall spatial distribution of discernible chromatin depleted regions corresponding to interphase chromosomes (Fig. 6b). The *in situ* DNase II matrix experiments confirmed the results from matrix preparations in solution. Eight- to 10-fold more

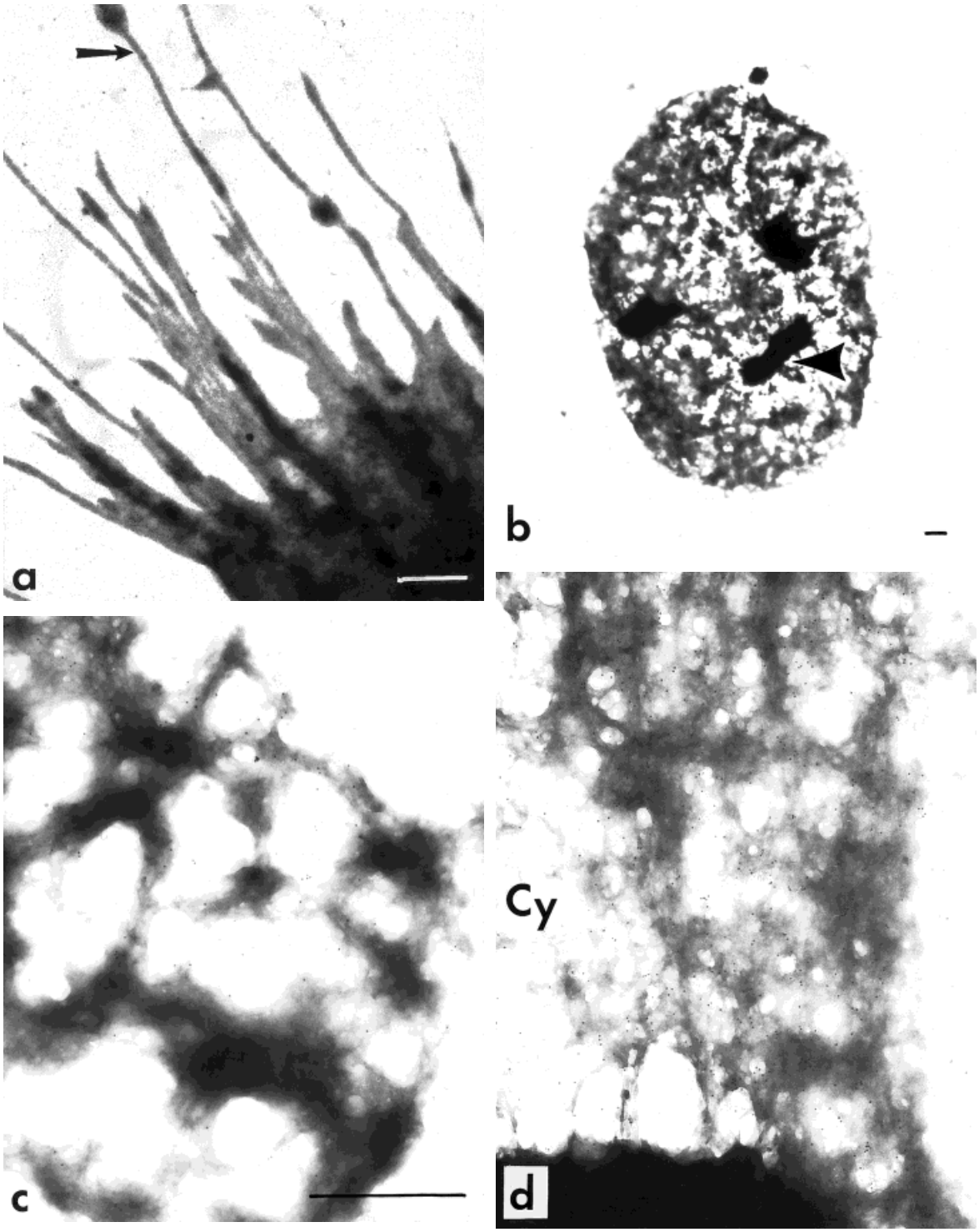

Fig. 6. Electron micrographs of in situ nuclear matrix preparations obtained from the DNase II procedure on grids. The cells attach well to the carbon and demonstrate phyllopodia (arrow) in the absence of detergent (**a**). The cell preserves its native nuclear architecture after this procedure (**b**), and only large-scale chromatin masses are removed, which might represent the interphase chromosomes. Three nucleoli are well discernible (arrowhead). When immunolabeling was performed, WT nuclear matrices were enriched in colloid bound to the meshwork (**c**), while SMR_{16} residual structures display mostly cytoplasmic (Cy) labeling (**d**). a,b: Scale bars represent 1 µm. c,d: Scale bar represents 0.1 µm.

topo IIα was associated with the *in situ* nuclear matrices from WT CHO cells (Fig. 6c) relative to matrices from SMR_{16} cells. In drug-resistant cells, the cytoskeletal meshwork was consistently labeled for topo IIα, while most of the nucleoskeletal structures present on the grid were not (Fig. 6d).

Immunofluorescent Microscopic Study of WT and SMR_{16} Cells

Immunofluorescence microscopy performed on intact cells that are grown on slides provides the most natural pattern of labeling, avoiding any redistribution of the topo IIα antigen. WT CHO cells have a topo IIα nuclear localization, which is dependent on low cell density (Fig. 7a). When WT CHO cells reach stable confluency, many of them translocate the enzyme to the cytoplasm or have no cytoplasmic or nuclear immunofluorescence for topo IIα (Fig. 7b). The existence of a cytoplasmic population of topo II with a COOH-end truncation and concomitant loss of nuclear localization signals is unlikely, as no bands of molecular mass less than 170 kDa were detected on numerous immunoblots for either WT or drug-resistant cells. The resistant cell line at all stages of growth possesses combined nuclear and cytoplasmic populations of the enzyme (Fig. 7c,d). The change in the proportion of labeling intensity of different compartments of the two cell lines is summarized in Table II.

These two lines also displayed a different potential for attachment; SMR_{16} cells adhere well to the slide, have a spindle-like shape, and have many flattened cells and numerous giant cells. The cell volume is 50% more than the parental cell line. This is reflected also in the radius of the derived nuclear matrices. Another characteristic of the drug-resistant cell line is the increased doubling time (14.2 vs. 17.8 h). No difference in the cell cycle distribution was detected by flow cytometry of log-phase cells of these cell lines [Sullivan et al., 1993].

As we focused on the interphase nucleoskeletons, we found that a good portion of the structural rearrangement of newly replicated chromatin is accomplished at that time. For that reason, the resistant cells, with a prolonged doubling time, have very frequent mitotic abnormalities and show delayed segregation of chromatids that may be due to lower decatenation activity. The parental cell line at anaphase displays a cytoplasmic fluorescence, surrounding the cluster of already resolved chromosomes (Fig. 8c,d), like that theoretically predicted [Duplantier et al., 1995] and observed for Chinese hamster cells [Petrov et al., 1993]. Another characteristic difference in topo IIα fluorescence was observed at late prophase, when WT cells clearly depict a ring-like arrangement of radially emanating chromatids embedded in a well-defined structure rich in topo IIα (Fig. 8a). SMR_{16} cells do not contain such a structure which may well contribute to a later defect in separating chromatids. Our studies demonstrated quite distinct patterns of abnormal mitotic distributions of topo IIα in SMR_{16} cells, showing that prolongation of anaphase chromatid separation is accompanied by a gradient of topo II fluorescence with a maximum at the separating unresolved chromosomes (Fig. 8e–h).

DISCUSSION

The morphology and biochemical characteristics of the nuclear matrix are dependent on the ionic strength during nuclear isolation, on the nucleases used, and on the protein extraction procedure. The core filaments of the nuclear matrix are sensitive to DNase I [Jackson and Cook, 1988], and their disruption by this nuclease is suggestive of participation of actin in this structure [He et al., 1990]. DNase I has also the disadvantage of dependence on divalent cations, which may activate phosphatases, proteases, poly(ADP)ribosylation and endogenous nucleases during the isolation procedure. Another procedure, which bypasses the artifacts caused by DNase I, employs DNase II and allows the procedure to be carried out in the presence of EDTA and thus avoids the side effects of divalent cations [Labhart et al., 1982]. Until now, this procedure allowed only the preservation of the lamina component [Krachmarov et al., 1986]. The internal nuclear matrix was observed only when heat-shock stabilization was performed [Krachmarov and Traub, 1993]. In order to preserve the RNP-containing inter-

Fig. 7. Immunofluorescent staining of Chinese hamster ovary cells grown on slides and labeled with the 454 antibody (specific for topo IIα) and visualized by rhodamine-conjugated antirabbit IgG. While WT cells maintain nuclear staining during log-phase growth (**a**) and acquire cytoplasmic labeling at confluency (**b**), SMR_{16} cells at the same time points have combined nuclear and cytoplasmic fluorescence (panels **c,d** are log-phase and confluent cells, respectively). DNA is stained by DAPI in the corresponding images (**a′–d′**). ×600.

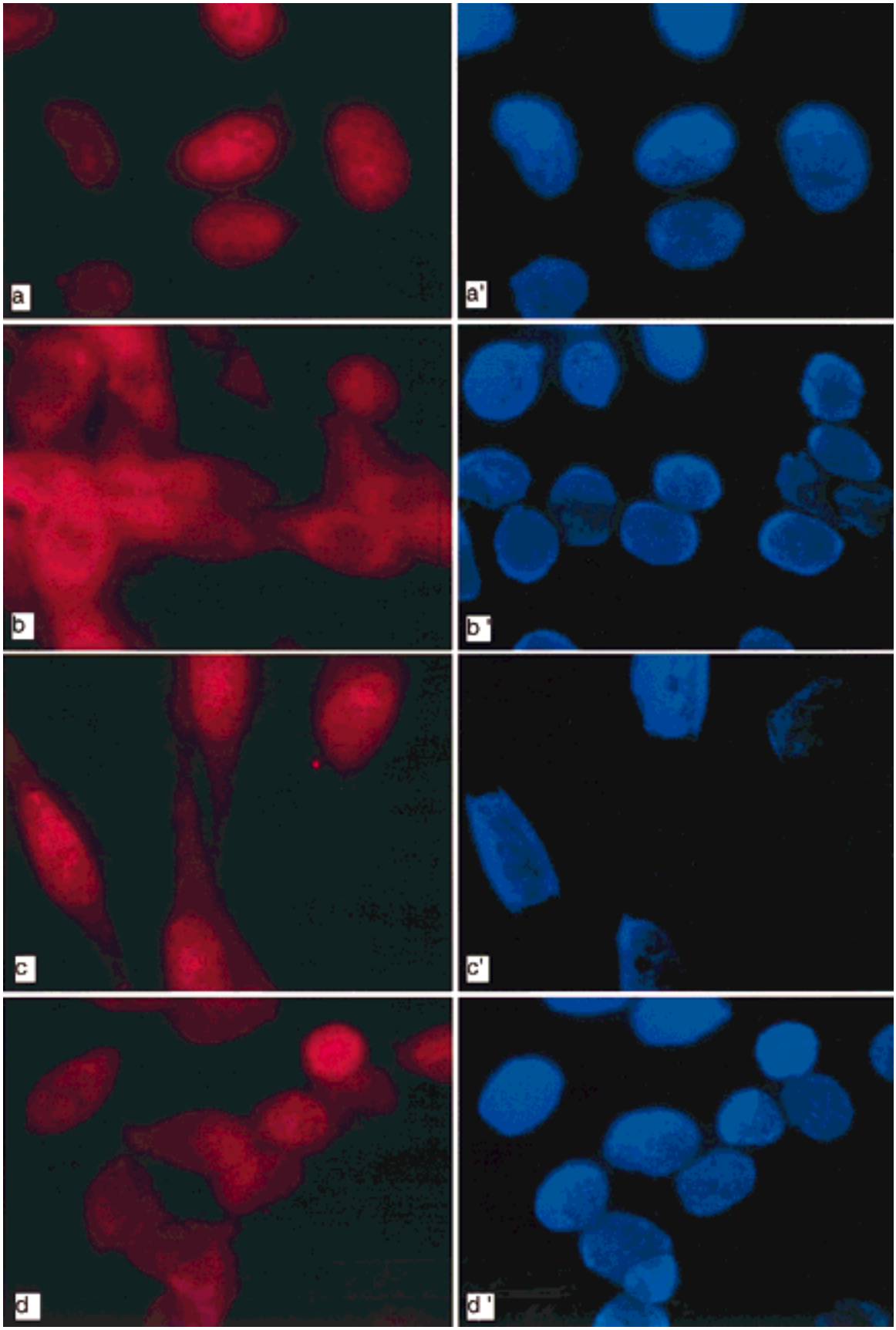

Figure 7.

TABLE II. Distribution Between the Cytoplasmic and Nuclear Compartments of the Immunofluorescent Staining Pattern of Topo IIα in WT and SMR_{16} Cells

	WT cells				SMR_{16} cells			
	1	2	3	4	1	2	3	4
Cell density ($\times 10^5$/ml)[a]	1.2	3.2	6.0	11.0	0.4	1.2	2.5	4.0
Topo IIα fluorescence[b]								
% negative	1	7	4	22	4	17	30	45
% cytoplasmic only	1	14	21	46	9	2	7	11
% nuclear only	81	74	63	2	48	49	28	7
% nuclear + cytoplasmic	13	4	10	29	38	30	27	36
% mitotic	4	1	2	1	1	2	8	1
Distribution of fluorescence[c]								
% nuclear	97.3	81.2	62.7	23.7	91.0	67.2	44.0	39.1
% cytoplasmic	2.7	18.8	37.3	76.3	9.0	32.8	56.0	60.9

[a]Cell densities obtained from trypsinizing and counting parallel slides. SMR_{16} cells are larger and plateau at a lower density. Time point 1, early log-phase; time point 2, mid log-phase; time point 3, late log-phase; time point 4, early plateau phase. Cell viability (by Trypan blue dye exclusion) was >95% at all time points.

[b]This is a qualitative assessment of cellular fluorescence; compartments were scored as either negative or positive. At least 200 cells were scored for each time point, and the entire experiment was repeated three times.

[c]This is a quantitative evaluation of topo IIα fluorescence. For example, for time point 1 for WT cells, 97.3% of the total topo IIα cellular fluorescence (measured in pixels) was found to be located in the nucleus (at least 200 cells were measured), while only 2.7% was in the cytoplasm. The experiment was repeated three times, and the same results (±5% error) were obtained.

nal nuclear matrix [Fey et al., 1986; He et al., 1991; Mattern et al., 1996], we omitted digestion with RNase in the nuclease digestion step. It has been shown that a RNA/nuclear matrix association is sensitive to topo II inhibitors [Schröder et al., 1987].

The protein extraction step is accomplished either by high salt (2 M NaCl or 250 mM $(NH_4)_2SO_4$), low salt (lithium diiodosalicylate), or polyanions (heparin/dextran sulphate). The possibility of artifactual precipitation of macromolecules into an unresolvable meshwork by rapid addition of the high salt is easily bypassed by gradually raising the salt concentration [Paulson, 1989]. An alternative approach to remove the digested chromatin is electroelution of agarose-encapsulated cells, but the method rarely removes more than 97% of chromatin. Recent data [Hempel and Strätling, 1996] show that with this method MAR (matrix-associated regions) and SAR (scaffold-associated regions) sequences are not matrix-bound. Thus, this approach has its artifacts as well.

Since the method of nuclear matrix preparation evidently determines the results obtained, we decided to explore the method that seems to be the most controlled. The observations that RNP structures are critical components of the internal nuclear matrix lead us to omit the RNase treatment, which was sufficient to preserve the "elusive" internal matrix under conditions generally considered unfavorable. The association of topo IIα with the nuclear matrix was examined in a protocol with chelating agent present and RNase absent. Previous attempts to trap topo II in the insoluble nucleoskeletal fraction were successful only after heat-shock stabilization, the presence of Ca^{++} and Cu^{++} at high concentrations [Lewis and Laemmli, 1982], or stabilization of intermolecular disulfide bonds [Kaufmann and Shaper, 1991; McConnell et al., 1987]. We found it unnecessary to stabilize topo II to the scaffolding structure; the presence of RNP seems to be the critical prerequisite, thus suggesting once more the existence of topo II–enriched RNP particles [Meller et al., 1994].

The quantity and subcellular distribution of topo IIα vary as a function of the proliferative state [Sullivan et al., 1987; Hsiang et al., 1988] or drug treatment [Wolverton et al., 1992]. The technical difficulties in detecting a high molecular weight polypeptide, tightly associated with DNA and chromatin, make studies highly dependent on the fixation and permeabilization protocols [Summer, 1996]. Factors such as cell density and substrate attachment may lead to an unexpected cytoplasmic location of topoisomerase II which is generally considered nuclear. This shuttling of a protein to different cellular compartments may well be a more general biological phenomenon [Smalheiser, 1996].

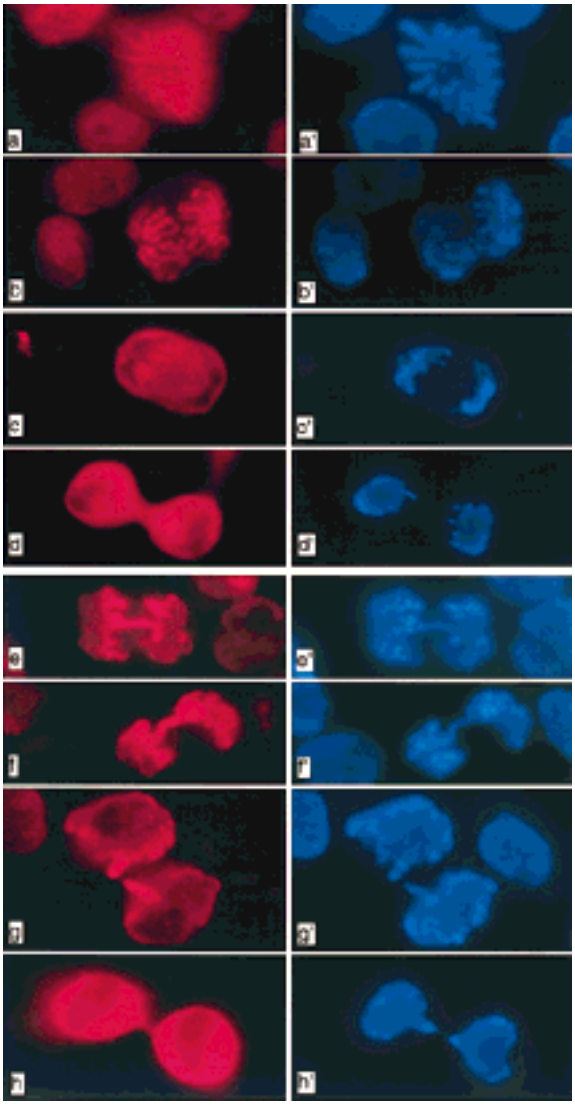

Fig. 8. Immunofluorescent staining for topo IIα of mitotic cells from WT and SMR_{16} cells. Mitotic WT cells have a metaphase chromosomal staining that in anaphase and telophase is converted to cytoplasmic fluorescence (**a–d**). SMR_{16} cells have a prolonged mitosis and maintain the chromosomal staining from metaphase (**e**) throughout anaphase and telophase with an apparent gradient distribution of topo IIα at late disjuncting chromosomes (**f–h**). DNA is stained by DAPI in the corresponding images (**a′–h′**). ×600.

The controlled digestion of chromatin DNA at pH 6.8 in the presence of EDTA enabled us to lower DNase II concentrations to 4 U/ml and to obtain matrix-associated DNA below 1% for the WT cell line. The resistant cell nuclear matrices retained four times more residual DNA, thus suggesting that the chromatin of SMR_{16} cells is less susceptible to the nuclease attack. This might be due to differences in chromatin structure induced by variable amounts of H1, polyamines, or higher order chromatin domain organization per se. Electron microscopy did reveal matrices possessing large halos, but the attached DNA loops were not accompanied by a greater quantity of topo II in the matrix, where the bases are supposed to be tethered by topo II molecules. In general, the quantities of residual DNA and topo II in individual nuclear matrices did not show a proportional relationship; they were in inverse proportion.

Our findings are not consistent with the widely accepted radial/loop model of chromatin organization and do not support a constant attachment of DNA loops to the nucleoskeleton via topo II. The quantity of topo IIα associated with the nuclear matrix appears to be highly dependent on the cell cycle stage and on the presence of RNP. The nucleoskeletal substructure by itself is highly dynamic, with a variable morphology of the fibrogranular components. The absence of any catalytic activity of the enzyme derived from the nuclear matrix is much more consistent with a storage-like function of the salt-stable matrix [Roberge et al., 1988; Fisher et al., 1989] than function as a site of DNA cleavage. A similar absence of topo IIα enzyme activity associated with the salt-resistant scaffold fraction was recently reported [Meyer et al., 1997]. The nuclear matrix more likely reflects active processes, taking place at the boundaries of chromatin and nonchromatin compartments of the living cell. The proximity of active topoisomerase II molecules to the underlying skeletal framework might be the explanation of the significant and reproducible depletion of the enzyme in drug-resistant cells in the nuclear matrix compared to the overall content in the cell. Under our conditions, the overall difference in topo II content in cells (1:2/3) was significantly different at the level of nuclear matrix (5–10:1). These studies suggest that nuclear matrix–associated topo II is intimately involved in the mechanism of drug resistance in SMR_{16} cells.

The ability to obtain nuclear matrix preparations *in situ*, and to visualize the matrix by whole-mount electron microscopy, is an approach aimed at minimizing possible artifacts. We decided to explore the possibility [de Graaf et al., 1991; Safiejko-Mroczka and Bell, 1996; Nickerson et al., 1997] of quickly fixing cells, thus ensuring that no redistribution of topo II occurs, and then proceeding with the nuclear

matrix procedure. Since DNase I has been reported to disrupt the core filaments of the nuclear matrix, DNase II seemed a logical alternative. Indeed, the controlled pH conditions of the procedure allowed a good digestion and extraction of the chromatin from briefly fixed cells, thus maximally preserving the underlying nucleoskeletal structure and its contact with the cytoskeletal framework. So far, only a few studies have demonstrated *in situ* whole-mount nuclear matrix preparations [Chew et al., 1993]. We adapted the DNase II procedure for our purposes and were successful in maximally preserving the nucleoskeleton *in situ*. The DNase II procedure employed in this study reliably demonstrates by immunoblotting, immunofluorescence, and immunoelectron microscopy that a perturbation in nuclear matrix–associated topo IIα is involved in the mechanism of drug resistance to topo II inhibitors in the SMR_{16} cell line.

The resolution of chromosomal DNA catenation, which results from replication, by topoisomerase II is supposed to occur at two stages: in S-phase and at metaphase/anaphase in the M-phase of the cell cycle. Anaphase bridging has been demonstrated in TOP2 mutants of *S. pombe* [Uemura et al., 1987]. In SMR_{16} cells we describe an analogous situation in mammalian cells that is due not to lack of enzyme but to its untimely association with the nuclear matrix during interphase with perhaps a defective S-phase, which leads to accumulation of disjunction defects in anaphase. Such an ability to bypass interphase defects in decatenation at mitosis was recently reported [Andreassen et al., 1997]. This phenomenon may contribute to drug resistance, since S-phase is considered an important stage for exerting the cytotoxic effects of topo II inhibitors by abolishing the propagation of the replication fork.

ACKNOWLEDGMENTS

It is a pleasure to thank Ed Haller for technical help with electron microscopy and many helpful suggestions.

REFERENCES

Andreassen PR, Lacroix FB, Margolis RL (1997): Chromosomes with two intact axial cores are induced by G_2 checkpoint override: Evidence that DNA decatenation is not required to template the chromosome structure. J Cell Biol 136:29–43.

Berrios M, Osheroff N, Fisher PA (1985): In situ localization of DNA topoisomerase II, a major polypeptide component of the *Drosophila* nuclear matrix fraction. Proc Natl Acad Sci U S A 82:4142–4146.

Birrell GB, Hedberg KK, Griffith OH (1987): Pitfalls of immunogold labeling: Analysis by light microscopy, transmission electron microscopy, and photoelectron microscopy. J Histochem Cytochem 35:843–853.

Burden DA, Goldsmith LJ, Sullivan DM (1993): Cell-cycle-dependent phosphorylation and activity of Chinese-hamster ovary topoisomerase II. Biochem J 293:297–304.

Chew EC, Yang L, Cheng-Chew SB, Leung PY, Jiao RJ, Zhai ZH (1993): Microwave fixation of nuclear matrix in tumor cells. Anticancer Res 13:2277–2280.

Cook PR (1988): The nucleoskeleton: Artefact, passive framework or active site? J Cell Sci 90:1–6.

Danks MK, Qui J, Catapano CV, Schmidt CA, Beck WT, Fernandes DJ (1994): Subcellular distribution of the α and β topoisomerase II–DNA complexes stabilized by VM-26. Biochem Pharmacol 48:1785–1795.

de Graaf A, van Bergen en Henegouven PMP, Meijne AML, van Driel R, Verkleij AJ (1991): Ultrastructural localization of nuclear matrix proteins in HeLa cells using silver-enhanced ultra-small gold probes. J Histochem Cytochem 39:1035–1045.

Drake FH, Zimmerman JP, McCabe FL, Bartus HF, Per SR, Sullivan DM, Ross WE, Mattern MR, Johnson RK, Crooke ST, Mirabelli CK (1987): Purification of topoisomerase II from amsacrine-resistant P388 leukemia cells: Evidence for two forms of the enzyme. J Biol Chem 262:16739–16747.

Duplantier B, Jannink G, Sikorav J-L (1995): Anaphase chromatid motion: Involvement of type II DNA topoisomerases. Biophys J 69:1596–1605.

Earnshaw WC, Halligan B, Cooke CA, Heck MMS, Liu LF (1985): Topoisomerase II is a structural component of mitotic chromosome scaffolds. J Cell Biol 100:1706–1715.

Feldhoff PW, Mirski SEL, Cole SPC, Sullivan DM (1994): Altered subcellular distribution of topoisomerase IIα in a drug-resistant human small cell lung cancer cell line. Cancer Res 54:756–762.

Fernandes DJ, Catapano CV (1991): Nuclear matrix targets for anticancer agents. Cancer Cells 3:134–140.

Fernandes DJ, Catapano CV (1995): The nuclear matrix as a site of anticancer drug action. Int Rev Cytol 162A:539–577.

Fernandes DJ, Smith-Nanni C, Paff MT, Neff T-AM (1988): Effects of antileukemia agents on nuclear matrix–bound DNA replication in CCRF-CEM leukemia cells. Cancer Res 48:1850–1855.

Fernandes DJ, Danks MK, Beck WT (1990): Decreased nuclear matrix DNA topoisomerase II in human leukemia cells resistant to VM-26 and m-AMSA. Biochemistry 29:4235–4241.

Fey EG, Krochmalnic G, Penman S (1986): The nonchromatin substructures of the nucleus: The ribonucleoprotein (RNP)-containing and RNP-depleted matrices analyzed by sequential fractionation and resinless section electron microscopy. J Cell Biol 102:1654–1665.

Fischer D, Hock R, Scheer U (1993): DNA topoisomerase II is not detectable on lampbrush chromosomes but enriched in the amplified nucleoli of *Xenopus* oocytes. Exp Cell Res 209:255–260.

Fisher PA (1989): Chromosomes and chromatin structure: The extrachromosomal karyoskeleton. Curr Opin Cell Biol 1:447–453.

Fisher PA, Lin L, McConnell M, Greenleaf A, Lee J-M, Smith DE (1989): Heat shock–induced appearance of RNA polymerase II in karyoskeletal protein-enriched (nuclear "matrix") fractions correlates with transcriptional shutdown in *Drosophila melanogaster.* J Biol Chem 264:3464–3469.

Harker WG, Slade DL, Parr RL, Feldhoff PW, Sullivan DM, Holguin MH (1995): Alterations in the topoisomerase IIα gene, messenger RNA, and subcellular protein distribution as well as reduced expression of the DNA topoisomerase IIβ enzyme in a mitoxantrone-resistant HL-60 human leukemia cell line. Cancer Res 55:1707–1716.

He D, Nickerson JA, Penman S (1990): Core filaments of the nuclear matrix. J Cell Biol 110:569–580.

He DC, Martin T, Penman S (1991): Localization of heterogeneous nuclear ribonucleoprotein in the interphase nuclear matrix core filaments and on perichromosomal filaments at mitosis. Proc Natl Acad Sci U S A 88:7469–7473.

Heck MMS, Earnshaw WC (1986): Topoisomerase II: A specific marker for cell proliferation. J Cell Biol 103:2569–2581.

Hempel K, Strätling WH (1996): The chicken lysozyme gene 5′ MAR and the *Drosophila* histone SAR are electroelutable from encapsulated and digested nuclei. J Cell Sci 109:1459–1469.

Hirano T, Mitchison TJ (1993): Topoisomerase II does not play a scaffolding role in the organization of mitotic chromosomes assembled in *Xenopus* egg extracts. J Cell Biol 120:601–612.

Hsiang Y, Wu H-Y, Liu LF (1988): Proliferation-dependent regulation of DNA topoisomerase II in cultured human cells. Cancer Res 48:3230–3235.

Jack RS, Eggert H (1992): The elusive nuclear matrix. Eur J Biochem 209:503–509.

Jackson DA (1991): Structure-function relationships in eukaryotic nuclei. Bioessays 13:1–10.

Jackson DA, Cook PR (1988): Visualization of a filamentous nucleoskeleton with a 23 nm axial repeat. EMBO J 7: 3667–3677.

Kaufmann SH, Shaper JH (1991): Association of topoisomerase II with the hepatoma cell nuclear matrix: The role of intermolecular disulfide bond formation. Exp Cell Res 192:511–523.

Krachmarov CP, Traub P (1993): Heat-induced morphological and biochemical changes in the nuclear lamina from Ehrlich ascites tumor cells in vivo. J Cell Biochem 52:308–319.

Krachmarov CP, Tasheva B, Markov D, Hancock R, Dessev G (1986): Isolation and characterization of nuclear lamina from Ehrlich ascites tumor cells. J Cell Biochem 30:351–359.

Labhart P, Koller T, Wunderli H (1982): Involvement of higher order chromatin structures in metaphase chromosome organization. Cell 30:115–121.

Lewis CD, Laemmli UK (1982): Higher order metaphase chromosome structure: Evidence for metalloprotein interactions. Cell 17:849–858.

Mattern KA, Humbel BM, Muijsers AO, de Jong L, van Driel R (1996): hnRNP proteins and B23 are the major proteins of the internal nuclear matrix of HeLa S3 cells. J Cell Biochem 62:275–289.

McConnell M, Whalen AM, Smith DE, Fisher PA (1987): Heat shock–induced changes in the structural stability of proteinaceous karyoskeletal in vitro and morphological effects in situ. J Cell Biol 105:1087–1098.

Meller VH, Fisher PA (1995): Nuclear distribution of *Drosophila* topoisomerase II is sensitive to both RNase and DNase. J Cell Sci 108:1651–1657.

Meller VH, McConnell M, Fisher PA (1994): An RNase-sensitive particle containing *Drosophila melanogaster* DNA topoisomerase II. J Cell Biol 126:1331–1340.

Meyer KN, Kjeldsen E, Straub T, Knudsen BR, Hickson ID, Kikuchi A, Kreipe H, Boege F (1997): Cell cycle–coupled relocation of types I and II topoisomerases and modulation of catalytic enzyme activities. J Cell Biol 136:775–788.

Miller OL, Bakken AH (1972): Morphological studies on transcription. Acta Endocrinol 168 (Suppl):155–173.

Mirski SEL, Cole SPC (1995): Cytoplasmic localization of a mutant M_r 160,000 topoisomerase IIα is associated with the loss of putative bipartite nuclear localization signals in a drug-resistant human lung cancer cell line. Cancer Res 55:2129–2134.

Nickerson JA, Krockmalnic G, Wan KM, Penman S (1997): The nuclear matrix revealed by eluting chromatin from a cross-linked nucleus. Proc Natl Acad Sci U S A 94:4446–4450.

Paulson JR (1989): Scaffold morphology in histone-depleted HeLa metaphase chromosomes. Chromosoma 97:289–295.

Penman S (1995): Rethinking cell structure. Proc Natl Acad Sci U S A 92:5251–5257.

Petrov P, Drake FH, Loranger A, Huang W, Hancock R (1993): Localization of DNA topoisomerase II in Chinese hamster fibroblasts by confocal and electron microscopy. Exp Cell Res 204:73–81.

Pienta KJ, Lehr JE (1993): Inhibition of prostate cancer growth by estramustine and etoposide: Evidence for interaction at the nuclear matrix. J Urol. 149:1622–1625.

Pienta KJ, Partin AW, Coffey DS (1989): Cancer as a disease of DNA organization and dynamic cell structure. Cancer Res 49:2525–2532.

Poljak E, Kas E (1995): Resolving the role of topoisomerase II in chromatin structure and function. Trends Cell Biol 5:348–354.

Qiu J, Catapano CV, Fernandes DJ (1996): Formation of topoisomerase IIα complexes with nascent DNA is related to VM-26–induced cytotoxicity. Biochemistry 35: 16354–16360.

Roberge M, Dahmus ME, Bradbury EM (1988): Chromosomal loop/nuclear matrix organization of transcriptionally active and inactive RNA polymerases in HeLa nuclei. J Mol Biol 201:545–555.

Safiejko-Mroczka B, Bell PB Jr (1996): Bifunctional protein cross-linking reagents improve labeling of cytoskeletal proteins for qualitative and quantitative fluorescence microscopy. J Histochem Cytochem 44:641–656.

Schröder HC, Trölltsch D, Friese U, Bachmann M, Müller WEG (1987): Mature mRNA is selectively released from the nuclear matrix by an ATP/dATP-dependent mechanism sensitive to topoisomerase inhibitors. J Biol Chem 262:8917–8925.

Smalheiser NR (1996): Proteins in unexpected locations. Mol Biol Cell 7:1003–1014.

Sullivan DM, Latham MD, Ross WE (1987): Proliferation-dependent topoisomerase II content as a determinant of antineoplastic drug action in human, mouse, and Chinese hamster ovary cells. Cancer Res 47:3973–3979.

Sullivan DM, Latham MD, Rowe TC, Ross WE (1989): Purification and characterization of an altered topoisomerase II from a drug-resistant Chinese hamster ovary cell line. Biochemistry 28:5680–5687.

Sullivan DM, Eskildsen LA, Groom KR, Webb CD, Latham MD, Martin AW, Wellhausen SR, Kroeger PE, Rowe TC (1993): Topoisomerase II activity involved in cleaving DNA into topological domains is altered in a multiple drug-resistant Chinese hamster ovary cell line. Mol Pharmacol 43:207–216.

Sumner AT (1996): The distribution of topoisomerase II on mammalian chromosomes. Chromosome Res 4:5–14.

Swedlow JR, Sedat JW, Agard DA (1993): Multiple chromosomal populations of topoisomerase II detected in vivo by time-lapse, three-dimensional wide-field microscopy. Cell 73:97–108.

Taagepera S, Rao PN, Drake FH, Gorbsky GJ (1993): DNA topoisomerase IIα is the major chromosome protein recognized by the mitotic phosphoprotein antibody MPM-2. Proc Natl Acad Sci U S A 90:8407–8411.

Uemura T, Ohkura H, Adachi Y, Morino K, Shiozaki K, Yanagida M (1987): DNA topoisomerase II is required for condensation and separation of mitotic chromosomes in *S. pombe*. Cell 50:917–925.

Wang X, Traub P (1991): Resinless section immunogold electron microscopy of karyo-cytoskeletal frameworks of eukaryotic cells cultured in vitro: Absence of a salt-stable nuclear matrix from mouse plasmacytoma MPC-11 cells. J Cell Sci 98:107–122.

Webb CD, Latham MD, Lock RB, Sullivan DM (1991): Attenuated topoisomerase II content directly correlates with a low level of drug resistance in a Chinese hamster ovary cell line. Cancer Res 51:6543–6549.

Wolverton JS, Danks MK, Granzen B, Beck WT (1992): DNA topoisomerase II immunostaining in human leukemia and rhabdomyosarcoma cell lines and their responses to topoisomerase II inhibitors. Cancer Res 52: 4248–4253.